

Cite this: *Mater. Horiz.*, 2019, 6, 1179Received 4th February 2019,  
Accepted 1st March 2019

DOI: 10.1039/c9mh00195f

rsc.li/materials-horizons

# Phenanthro[9,10-*d*]triazole and imidazole derivatives: high triplet energy host materials for blue phosphorescent organic light emitting devices†

Muazzam Idris,<sup>a</sup> Caleb Coburn,<sup>b</sup> Tyler Fleetham,<sup>a</sup> JoAnna Milam-Guerrero,<sup>a</sup> Peter I. Djurovich,<sup>a</sup> Stephen R. Forrest\*<sup>bcd</sup> and Mark E. Thompson<sup>id</sup>\*<sup>a</sup>

**A class of wide bandgap host materials is introduced as an alternative to carbazole-based hosts to enhance the efficiency and transport properties of organic light emitting diodes (OLEDs). We have synthesized and investigate the photophysical and electrochemical properties of a series of phenanthrene derivatives incorporating fused triazole or imidazole rings. The resulting phenanthro[9,10-*d*]triazoles and phenanthro[9,10-*d*]imidazoles are suitable host materials for blue phosphors due to their high triplet energies and conductivities. Incorporation of bulky substituent groups leads to retention of the high triplet energies in the solid state. The most promising materials are incorporated in blue phosphorescent OLEDs that achieve external quantum efficiencies > 20%.**

## Introduction

Organic  $\pi$ -conjugated materials have attracted significant attention in the field of optoelectronics, due to their tunable photophysical and electrochemical properties and facile syntheses.<sup>1</sup> Understanding the relationship between material structures and their properties is crucial in developing materials with desired photophysical, electrochemical, and thermal properties for application in organic light emitting diodes (OLEDs),<sup>2</sup> organic photovoltaics,<sup>3</sup> organic field-effect transistors,<sup>4</sup> molecular sensors and non-linear optics.<sup>5</sup> Over the past few years, OLEDs have

### Conceptual insights

There are a limited number of materials with sufficiently high triplet energies to host blue phosphorescent emitters in organic light emitting diodes. Among them, carbazole-based core structures stand out due to their good transport properties. The phenanthro[9,10-*d*]imidazole core also has a high triplet energy, but green and red emitters using phenanthro[9,10-*d*]imidazoles hosts are reported to have only moderate efficiencies, and have very low efficiencies when used with blue emitters. The low efficiency is mainly due to low triplet energies of the phenanthro[9,10-*d*]imidazole in the solid state. Here, we introduce high energy host materials based on both phenanthro[9,10-*d*]imidazole and phenanthro[9,10-*d*]triazole cores, using aryl and heteroaryl substituents to retain their high triplet energy in the solid state. The phenanthro[9,10-*d*]imidazole gives a high blue phosphorescent OLED efficiency. Thus, the phenanthro[9,10-*d*]imidazole core serves as an alternative to carbazoles for achieving high triplet energies useful as hosts for blue phosphors.

attracted considerable attention for full color displays and solid-state lighting.<sup>6</sup> This interest is due in large part to the development of transition metal complexes as phosphorescent emitters, making it possible to harvest both singlet and triplet excitons, thereby achieving nearly 100% electroluminescence quantum efficiency.<sup>7</sup>

To achieve high OLED efficiency, a phosphorescent emitter is typically doped into a host matrix to suppress concentration quenching and triplet-triplet/triplet-polaron annihilation, while promoting transfer of charge and/or excited states onto the phosphor.<sup>8</sup> The host material requires a triplet energy ( $E_T$ ) higher than that of the phosphorescent dopant to ensure exclusive emission from the dopant. Hosts for green and red phosphors have been developed, leading to highly efficient and long-lived OLEDs. However, there is a dearth of stable host-guest systems with high triplet energies and appropriate frontier orbital energy levels for charge injection and transport for blue OLEDs. In particular, the high triplet energy required for blue OLED hosts limits molecular design to rigid, non-conjugating building blocks with triplet energies approaching 3 eV, such as fluorene, carbazole (cz), dibenzothiophene (dbt) and dibenzofuran (dbf),

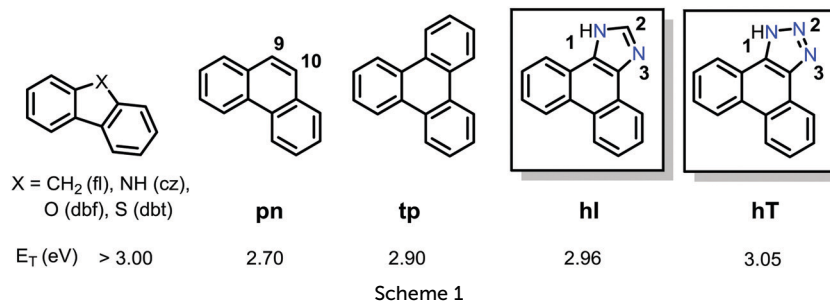
<sup>a</sup> Department of Chemistry, University of Southern California, Los Angeles, California 90089, USA. E-mail: met@usc.edu

<sup>b</sup> Department of Physics, University of Michigan, Ann Arbor, Michigan 48109, USA. E-mail: stevefor@umich.edu

<sup>c</sup> Department of Electrical and Computer Engineering, University of Michigan, Ann Arbor, Michigan 48109, USA

<sup>d</sup> Department of Materials Science and Engineering, University of Michigan, Ann Arbor, Michigan 48109, USA

† Electronic supplementary information (ESI) available: Experimental procedures and methods. Photophysical data of the host materials. Cyclic voltammetry curves, differential pulse voltammetry, calculated frontier molecular orbitals, DSC and TGA heating curves of the host materials. Hole and electron only  $J-V$  characteristics of FIrpic devices with the host materials. See DOI: 10.1039/c9mh00195f



see Scheme 1. Carbazole-based host materials stand out, due to their high PHOLED efficiencies when combined with blue phosphors.<sup>1b,9</sup> In contrast, the triplet energy of phenanthrene (**pn**, Scheme 1) is too low for this purpose, and thus has only seen limited use in blue host materials.<sup>10</sup> However, annulation of a five or six membered ring on the 9,10-positions of the phenanthrene ring increases the triplet energy to levels approaching 3 eV. For example, phenanthro[9,10-*d*]imidazole (**hl**) and triphenylene (**tp**) have triplet energies of up to 2.9 eV. Unfortunately, host materials containing **hl** and **tp** cores give only moderate efficiency when paired with green, yellow, red triplet emitters,<sup>11</sup> and very low efficiency with blue emitters.<sup>12</sup> These poor efficiencies are due to a marked lowering of  $E_T$  in neat solids relative to their  $E_T$  in solution. Therefore, we considered whether alternative phenanthrene-cored systems could serve as high triplet energy host materials with high solid-state  $E_T$ .

In previous work, we used computational methods to screen several phenanthrene derivatives with pyrrole, triazole, imidazole, furan and thiophene fused at the 9,10-positions of phenanthrene. Derivatives with the phenanthro[9,10-*d*]triazole (**hT**) and phenanthro[9,10-*d*]imidazole (**hl**) cores emerged as structures that have the highest triplet energies.<sup>13</sup> Here, we describe a series of phenanthro[9,10-*d*]triazole and phenanthro[9,10-*d*]imidazole based materials, and identify structures that have high triplet energies

as neat solids. Optimized syntheses of these materials, their photophysical and electrochemical properties, and a strategy to inhibit aggregation induced red-shifts to retain high triplet energies in a neat solid are discussed. The most promising materials are incorporated as host materials for blue phosphorescent OLEDs with > 20% external quantum efficiency.

## Results and discussion

A range of different phenanthro[9,10-*d*]triazole and phenanthro[9,10-*d*]imidazole based materials were prepared to investigate the electronic and thermal properties as a function of the substituents on the triazole and imidazole rings (Fig. 1). Alkyl triazoles were prepared from 9-bromo phenanthrene in two steps. The benzyne click chemistry (first step) is reported elsewhere.<sup>14</sup> The subsequent alkylation step was carried out in a one pot reaction of **hT** with K<sub>2</sub>CO<sub>3</sub> and methyl iodide. This reaction yielded predominantly the N2-isomer (**2-MeT**, 44%) and a minor amount of the N1 isomer (**1-MeT**, 25%), presumably due to steric interactions between the methyl group and the neighboring proton of the phenanthrene.

Aryl-substituted triazoles were prepared using modified procedures of Ueda *et al.* and Taillefer *et al.* who reported Ullman conditions for arylation of benzo-triazole.<sup>15</sup> Ullman conditions



Fig. 1 Structures of phenanthro[9,10-*d*]imidazoles and triazoles.

using **hT** and phenyl halide resulted in **2-pT** as the only product in 60% yield. The same result with slightly lower yield was obtained when Buchwald conditions were employed.<sup>15a</sup> The larger size of the phenyl ring is the likely reason that only the aryl N2 isomer is obtained. Therefore, N1 aryl substituted triazoles were prepared *via* a modified fluoride-induced elimination to generate benzyne under mild conditions.<sup>16</sup> This procedure produced N1 aryl substituted triazoles **1-pT**, **mT**, **mxT**, **fxT** and **txT** in 40–50% yields. A key modification from the literature procedure is preparation of 9-hydroxyphenanthrene using *n*-BuLi instead of Mg tunings,<sup>15a</sup> which gives the product in higher yield, with fewer byproducts and shorter reaction times. Phenanthro[9,10-*d*]imidazoles **MeI**, **pI**, **mI**, **mxI**, **fxI**, **txI** and **tpI** were prepared from inexpensive starting material (9,10-phenanthrenequinone) from two high yielding steps.<sup>12</sup>

### Targeting materials as blue OLED hosts

The study of the properties of these phenanthrene-based materials started with simple structures, aimed at characterizing the phenanthro-triazole and -imidazole core structures. While our theoretical modeling identified phenanthro-triazole and -imidazole based materials with high triplet energies, they also showed that it was not possible to predict which compounds would make the best host materials without detailed and time consuming modeling in the solid state.<sup>13</sup> Moreover, the modeling does not provide the bulk thermal properties of the materials, which is important in making stable OLEDs. Thus, we prepared a number of phenanthro-triazole and -imidazole based materials to identify those structures possessing the desired electronic and thermal properties for viable host materials for blue phosphorescent OLEDs.

Absorption spectra of the methyl substituted phenanthro-triazole and -imidazole materials were recorded in 2-MeTHF, Fig. 2a. The lowest energy band of the phenanthro-triazoles are blue-shifted by about 15 nm compared to a similar band of the phenanthro-imidazoles. The properties of the molecules depend on the site of the phenyl substitution. Phenyl substituents at the

1-position of either the triazole- or imidazole-based materials do not lead to a red shift, relative to the methyl substituted analogs (see Fig. S1, ESI<sup>†</sup>). Steric interactions force the phenyl ring at the 1-position to be out of plane with phenanthro- core and thus disrupts conjugation between the two aromatic ring systems. In contrast, a phenyl substituent at the 2-position adopts a coplanar conformation with the phenanthro[9,10-*d*]triazole core, leading to conjugation and a red-shift of *ca.* 30 nm relative to the analogous 1-phenyl substituted compounds. The same red shift has been observed for analogous phenyl substitution on phenanthro[9,10-*d*]imidazole.<sup>13</sup> Thus, substitution at the 1-position in these phenanthro-based materials was chosen to maintain high exciton energy.

The fluorescent ( $S_1$ ) and phosphorescent ( $T_1$ ) transitions of the triazoles are blue-shifted relative to their imidazole analogs (*e.g.* compare **1-MeT** to **MeI**, Fig. 2b and c). The triplet energies of **1-MeT** and **MeI** in solution are high ( $E_T = 2.97$  and 2.89 eV, respectively); however, the planar structures of **1-MeT** and **MeI** lead to aggregation in thin films, lowering their triplet energies to 2.66 eV and 2.70 eV, respectively (Fig. 2d). The PL efficiency of iridium(III)bis((4,6-difluorophenyl)pyridinato-*N,C2'*)picolinate (FIrpic), a blue phosphorescent emitter ( $E_T = 2.70$  eV),<sup>17</sup> doped into a **1-MeT** film is low (PLQY < 20%). A higher efficiency is observed for FIrpic doped into **MeI** (PLQY = 60%), but both hosts fall short of the 80% efficiency observed for FIrpic doped into polystyrene ( $E_T = 3.2$  eV).<sup>18</sup>

Aryl substituents at the 1-position in the triazole and imidazole compounds lead to higher triplet energies in the solid-state ( $E_{T\text{solid}}$ ) since the out-of-plane conformation of the aryl groups hinders  $\pi$ - $\pi$  stacking in the condensed phase. The triplet energy of the triazole with a phenyl group at the N1-position (**1-pT**,  $E_{T\text{solid}} = 2.75$  eV) is higher than that of **1-MeT** ( $E_{T\text{solid}} = 2.67$  eV), whereas the values for the imidazole analogs, **pI** and **MeI**, are the same ( $E_{T\text{solid}} = 2.70$  eV). To further inhibit aggregation-induced redshifts, mesityl groups were incorporated at the N1-positions of the triazole and imidazole compounds. The resultant materials, **mT** and **mI**, have high triplet

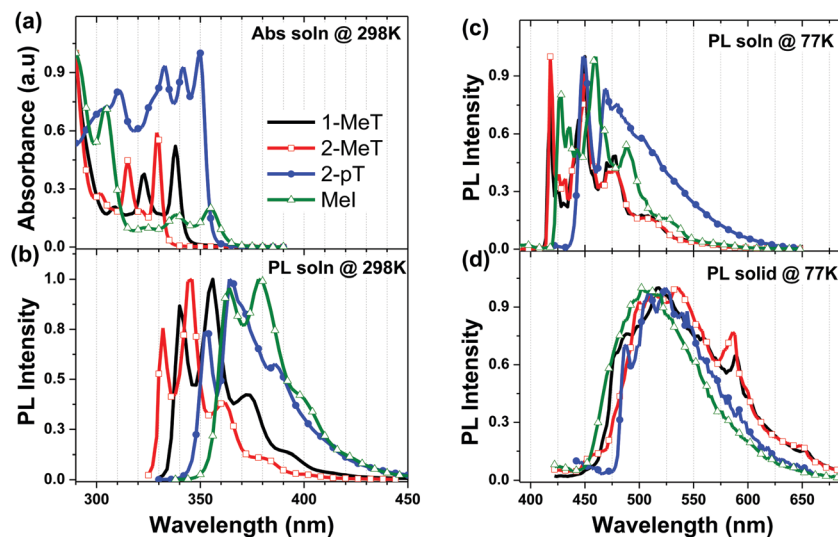


Fig. 2 (a) Absorption spectra in 2-MeTHF at 298 K. Normalized emission spectra in 2-MeTHF at 298 K (b) and 77 K (c), and as a neat solid at 77 K (d).

energies ( $E_{T_{\text{solid}}} = 2.77$  eV and 2.74 eV, respectively) and the PL efficiencies of FIrpic doped into films of both compounds are correspondingly increased (PLQY = 80%).

In addition to maintaining a high triplet energy in the solid state, it is important for a host material to have high sublimation ( $T_s$ ) and glass transition ( $T_g$ ) temperature for stable OLED performance. Thermogravimetric analysis showed that **mT** and **mI** have  $T_s < 300$  °C, due to their low molecular weight. No  $T_g$  was observed for **mT**, whereas the value for **mI** is too low ( $T_g = 72$  °C) for OLED applications. Derivatives with a mesityl-*o*-xylyl group at the N1-position (**mxT** and **mxI**) were prepared with increased  $T_s$  of 326 °C and  $T_g$  of 94 °C. As expected, **mxT** and **mxI** have the same energies for the  $S_1$  and  $T_1$  states (Fig. 3) as **mT** and **mI** (Fig. S2, ESI<sup>†</sup>). The mesityl-*o*-xylyl group also raises the triplet energy of **mxT** in the solid-state ( $E_{T_{\text{solid}}} = 2.77$  eV) relative to **1-MeT** ( $E_{T_{\text{solid}}} = 2.67$  eV) due to inhibited  $\pi$ - $\pi$  interactions, although not for **mxI** relative to **MeI** (Fig. 3a and b).

Dibenzofuran (dbf) and dibenzothiophene (dbt) groups are often used in host materials with high triplet energies. Here, these groups were used to further improve the thermal properties of the phenanthro-triazole and phenanthro-imidazole compounds. The triplet energies for **fxT**, **txT**, **fxI** and **txI** are similar to **mxT** and **mxI**, but the dbf and dbt based compounds have higher sublimation ( $T_s > 390$  °C) and glass transition ( $T_g = 125$ – $130$  °C) temperatures (Table 1). Coupling the dbf and dbt groups to the phenanthro-triazole or -imidazole core through a *p*-xylyl group proved to be important. If the *p*-xylyl ring is replaced with a

phenyl group, *i.e.* **tpI**, conjugation between dbt and phenanthroimidazole substantially lowers the triplet energy ( $E_{T_{\text{solid}}} = 2.64$  eV). However, placing the *p*-xylyl spacer between dbt or dbf on **fxT**, **txT**, **fxI** and **txI** allowed these materials to retain high triplet energies in both solution and the solid-state ( $E_{T_{\text{solid}}} > 2.75$  eV).

### Frontier orbital energies

The electrochemical properties of the phenanthro-triazole and -imidazole compounds were characterized using cyclic voltammetry (CV) and differential pulse voltammetry (DPV). Data for selected compounds are given in Table 1. Phenanthro-triazoles show irreversible oxidation and quasi-reversible reduction (scan rates of 0.1 V s<sup>-1</sup> and 10 V s<sup>-1</sup>) with the exception of **1-MeT** and **2-pT**, which show reversible reductions (see Fig. S12, ESI<sup>†</sup>). Phenanthro-imidazoles have quasi-reversible oxidation and reversible reductions. The phenanthro-triazoles oxidize in the range of 1.42–1.45 V vs. Fc<sup>+</sup>/Fc, whereas the phenanthro-imidazoles are cathodically shifted by roughly 400 mV ( $E_{\text{ox}} = 1.0$ – $1.05$  V). The reduction potentials for the phenanthro-triazoles are similarly shifted by 250 mV relative to those of the imidazole-based materials ( $E_{\text{red}} = -2.69$  and  $-2.96$  V, respectively). The anodic shift for both oxidation and reduction of triazoles relative to their imidazole-based counterparts is due to replacement of carbon with more electro-negative nitrogen atom in the triazoles, stabilizing both the HOMO and the LUMO. The HOMO and LUMO energies in Table 1 were estimated from the measured oxidation and reduction potentials.<sup>19</sup> The wide HOMO/LUMO gaps of these

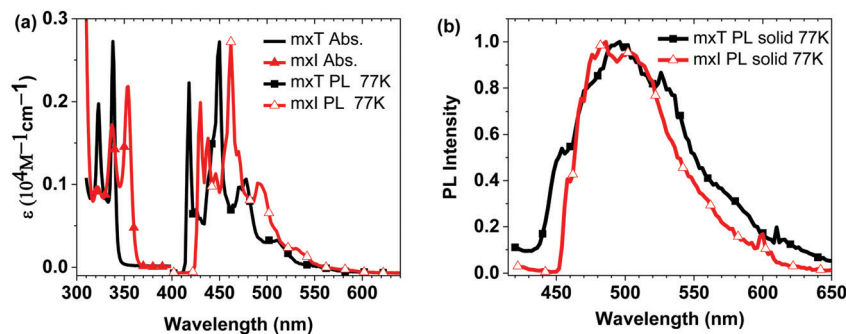


Fig. 3 (a) Absorption spectra and normalized emission spectra in 2-MeTHF at 77 K. (b) Normalized emission spectra in neat solid at 77 K.

Table 1 Summary of properties for selected phenanthro-triazoles and -imidazoles

| Compound    | $S_1^a$ (eV) | $E_T$ (eV)         |                    | $E_{\text{ox}}^d$ (V) | $E_{\text{red}}^d$ (V) | HOMO/LUMO <sup>e</sup> (eV) | $T_g/T_m/T_s^f$ (°C) |
|-------------|--------------|--------------------|--------------------|-----------------------|------------------------|-----------------------------|----------------------|
|             |              | Soln. <sup>b</sup> | Solid <sup>c</sup> |                       |                        |                             |                      |
| <b>mT</b>   | 3.65         | 2.97               | 2.77               | +1.44                 | -2.69                  | -6.45/-1.66                 | —/263/293            |
| <b>mxT</b>  | 3.65         | 2.97               | 2.77               | +1.42                 | -2.73                  | -6.42/-1.61                 | 94/247/326           |
| <b>fxT</b>  | 3.65         | 2.97               | 2.75               | +1.45                 | -2.67, -3.03           | -6.46/-1.68                 | 126/237/398          |
| <b>txT</b>  | 3.65         | 2.97               | 2.70               | +1.45                 | -2.64, -3.00           | -6.46/-1.71                 | 128/219/398          |
| <b>mI</b>   | 3.45         | 2.89               | 2.74               | +1.00                 | -2.96                  | -5.94/-1.34                 | 72/171/294           |
| <b>mxI</b>  | 3.45         | 2.89               | 2.73               | +1.05                 | -2.98                  | -6.00/-1.31                 | 94/196/326           |
| <b>fxI</b>  | 3.45         | 2.89               | 2.71               | +1.00                 | -2.95, -3.06           | -5.94/-1.35                 | 126/—/376            |
| <b>txI</b>  | 3.45         | 2.89               | 2.74               | +1.01                 | -2.93, -3.04           | -5.95/-1.37                 | 130/212/396          |
| <b>mCBP</b> | 3.60         | 2.93               | 2.86               | +0.88                 | -2.84                  | -5.80/-1.48                 | —                    |

<sup>a</sup> Measured in 2-MeTHF at 298 K. <sup>b</sup> Measured in 2-MeTHF at 77 K. <sup>c</sup> Onset of the triplet emission for the neat powder at 77 K. <sup>d</sup> Obtained from differential pulse voltammetry (DPV) in acetonitrile vs. Fc<sup>+</sup>/Fc. <sup>e</sup> Calculated from redox values according to ref. 19. <sup>f</sup>  $T_g$  = glass transition temperature,  $T_m$  = melting point,  $T_s$  = sublimation temperature under nitrogen.

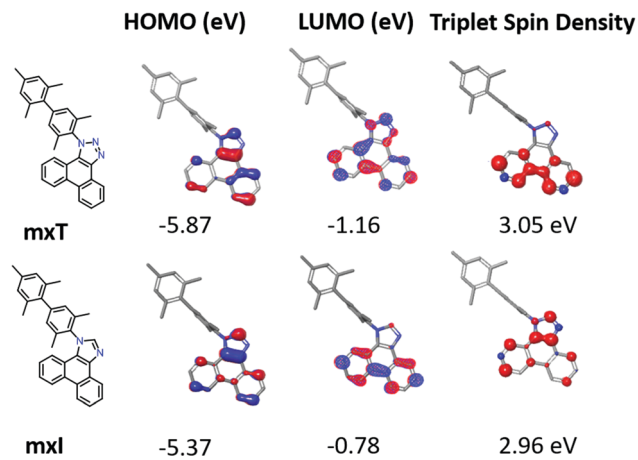


Fig. 4 Frontier molecular orbitals and triplet spin density of **mxT** and **mxI**.

materials make them suitable for hosting blue phosphorescent dopants such as FIrpic ( $E_{\text{ox}} = 0.92$  V,  $E_{\text{red}} = -2.29$  V).<sup>20</sup>

The electronic properties of the phenanthro-triazoles and -imidazoles were also investigated theoretically using density functional and time dependent density functional theory. Geometry optimization in the gas phase was performed using B3LYP functional with an LACVP\*\* basis set. Contours representative for the valence molecular orbitals (MOs) of phenanthro-triazoles and -imidazoles are shown for **mxT** and **mxI** in Fig. 4. The HOMO is localized on the phenanthro-triazole/imidazole ring for all compounds, consistent with the small variation in  $E_{\text{ox}}$  within each phenanthro-triazole and phenanthro-imidazole series. The LUMO is localized on the phenanthro-triazole/imidazole ring for **mxT** and **mxI**. In contrast, the LUMO is localized on the dbf moiety in **fxT** and **fxI** or dbt moiety in **txT** and **txI** whereas, the LUMO+1 is localized on the phenanthro-triazole or -imidazole moiety. The electrochemical data for **fxT**, **fxI**, **txT** and **txI**, however, suggest that the first reduction occurs on the phenanthro-triazole or -imidazole moiety, and the second reduction on the dbf or dbt moiety (Table 1 and Fig. S13, ESI†). These contrasting results are likely due to similar energies for the calculated LUMO and LUMO+1 of **fxT**, **fxI**, **txT** and **txI**. (see Fig. S15 and 16, ESI†).

The triplet energies calculated for the phenanthro-triazoles are 3.05 eV and 2.95 eV for phenanthro-imidazoles. These values are similar to the experimental values of 2.97 eV for the triazoles and 2.90 eV for the imidazoles. The triplet spin density for the N1-substituted phenanthro-triazoles and -imidazoles is localized on the phenanthro-triazole/imidazole core (Fig. 4). Exceptions are **2-pT** and **fxT**. In **2-pT** the triplet spin density delocalizes over the entire phenyl-phenanthro-triazole, stabilizing the triplet at 2.80 eV (measured = 2.75 eV). The triplet density of **fxT** is localized on the dbf moiety (Fig. S16, ESI†) due to the similar energies of dbf ( $T_1 = 3.13$  eV) and phenanthro-triazole core ( $T_1 = 3.06$  eV).

### Electroluminescence properties

The photophysical, electrochemical and thermal properties of selected phenanthro-triazoles and -imidazoles are summarized in Table 1. All of the listed compounds have suitable electronic

properties to host blue phosphorescent OLEDs. The thermal properties of **mT** and **mI** are unsuitable for OLED applications, so they were not considered further. Materials with high triplet energies in the solid-state and good thermal properties were incorporated as host materials in blue OLED.

In the first set of experiments, a direct comparison was made of OLEDs with phenanthro-triazole and -imidazole hosts, *i.e.* **mxT** and **mxI**, doped with FIrpic (see ESI† for device details and Fig. S17 for device performance). Whereas the triazole and imidazoles based devices exhibit similar current density–voltage ( $J$ – $V$ ) characteristics and electroluminescence (EL) spectra, devices using **mxT** hosts degrade rapidly under EL operation, with second and third  $J$ – $V$  scans ( $0.01$ – $100$  mA cm<sup>-2</sup>) showing a >75% drop in efficiency (Fig. S17, ESI†). For comparison the EQE for the imidazole based device drops <10% with the same current cycling. The rapid decrease in efficiency for the **mxT** based device is likely due to degradation of the phenanthro[9,10-*d*]triazole host materials, which could be caused by the irreversibility to electrochemical oxidation or reduction. All device testing was done with devices packaged under dry nitrogen. Rapid decay in EQE at high current density is observed with the other phenanthro-triazole devices as well (**fxT** and **txT**, Fig. S18, ESI†). It should be noted that this sort of cycling to high current is not a direct indication of the device lifetime, yet the behavior of **mxT** clearly shows an inherent instability for the triazole based materials. We therefore subsequently focus on imidazole based materials.

In Fig. 5 we compare the performance of OLEDs using the three phenanthro-imidazole based host materials, as well as analogous devices with two conventional host materials (**mCBP** and **26DCzppy**), see Table 2 for device metrics. The device structure is illustrated in Fig. 5. The **mCBP** and phenanthro-imidazole derivatives have similar  $J$ – $V$  characteristics, whereas the **26DCzppy** shows a shift to higher voltage, Fig. 5a. The electroluminescence (EL) spectra, shown in Fig. 5b, are independent of the host material and are stable under repeated electrical excitation. The transport properties of these materials were further investigated using hole- and electron-only devices (Fig. S20, ESI†). The  $J$ – $V$  characteristics of these single carrier devices are largely independent of the host, with **mCBP** devices showing  $6 \pm 3\%$  and  $15 \pm 4\%$  lower voltages at 10 mA cm<sup>-2</sup> for electron- and hole-only devices, respectively, compared to the phenanthro-imidazole host devices. The phenanthro-imidazole and reference hosts devices exhibit similar brightness at low current densities with slight differences at higher current densities (Fig. 5d). OLEDs with the **txI** host give the highest efficiency (peak EQE =  $20.2 \pm 0.3\%$ , CE =  $43.9$  cd A<sup>-1</sup>), whereas OLEDs utilizing **fxI** and **mxI** hosts give slightly lower efficiencies (19%) (Fig. 5c and Table 2). The efficiency of devices employing **txI** is higher than **fxI** and **mxI** is due to higher triplet energy of **txI** in the solid-state than that of the latter compounds. This could be due to slightly larger size of dbt unit in **txI** than dbf unit in **fxI** or mesityl unit in **mxI** which helps to reduce aggregation-induced redshift of **txI** in the solid state. The **mCBP** host device efficiency is marginally lower with a peak EQE =  $16.7 \pm 0.5\%$  and CE =  $39.0$  cd A<sup>-1</sup>.

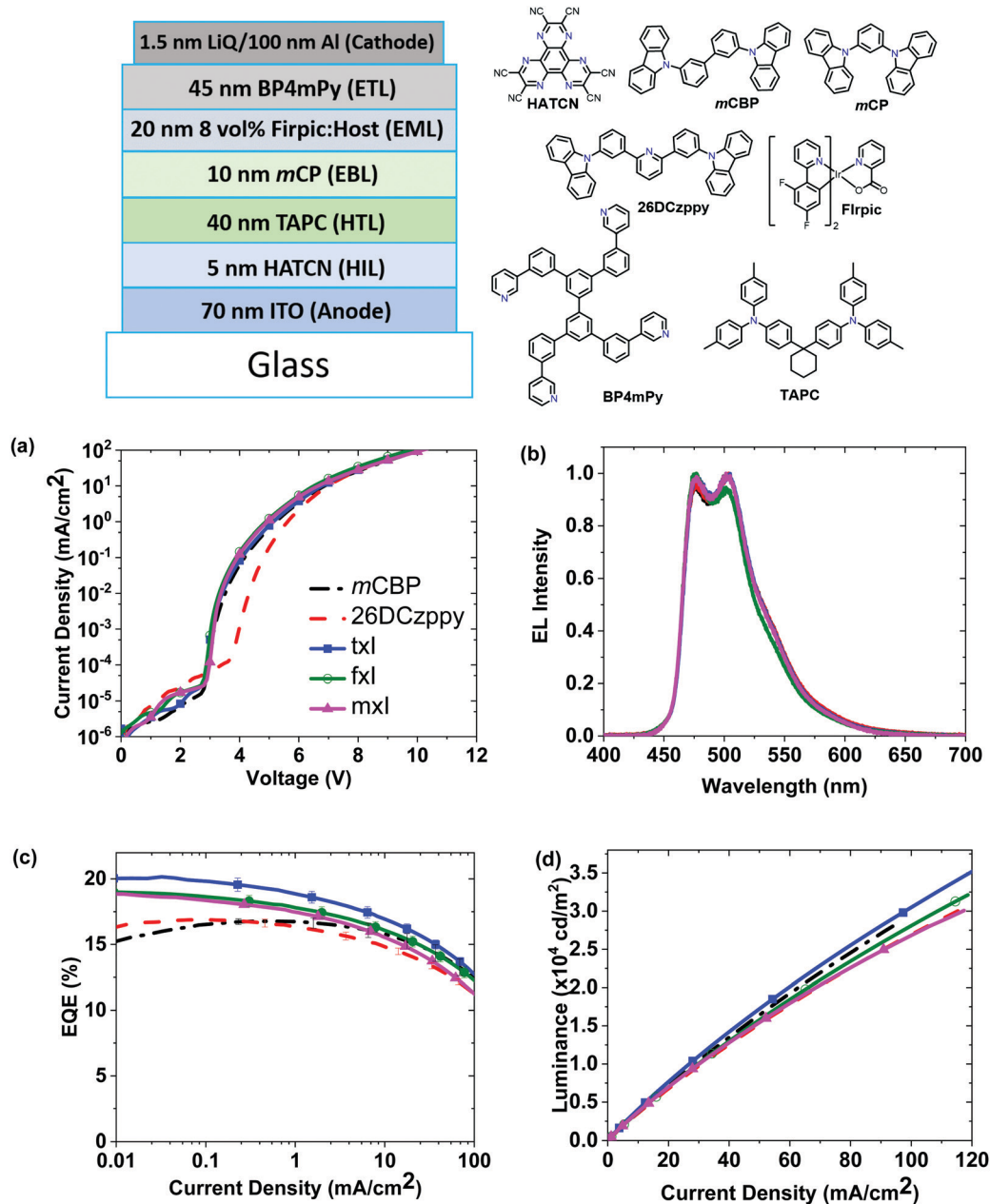


Fig. 5 OLED device characteristics of phenanthro[9,10-*d*]imidazole and reference hosts. (top) Device architecture and chemical formula of materials. (a)  $J-V$  curves. (b) EL spectra. (c) Efficiency versus current curves. (d) Luminance versus current curves.

Table 2 PLQY and EL properties of host materials

| Host     | PLQY <sup>a</sup><br>(%) | EQE <sub>max</sub><br>(%) | $V_{\text{on}}^b$<br>(V) | CE ( $\text{cd A}^{-1}$ )  |                             |                               |
|----------|--------------------------|---------------------------|--------------------------|----------------------------|-----------------------------|-------------------------------|
|          |                          |                           |                          | @100<br>$\text{cd m}^{-2}$ | @1000<br>$\text{cd m}^{-2}$ | @10 000<br>$\text{cd m}^{-2}$ |
| mxl      | 77                       | 19                        | 3.2                      | 43.1                       | 40.3                        | 33.2                          |
| fxl      | 66                       | 19                        | 3.1                      | 42.1                       | 39.4                        | 33.7                          |
| txl      | 77                       | 20                        | 3.1                      | 46.8                       | 43.9                        | 37.2                          |
| mCBP     | 87                       | 17                        | 3.3                      | 40.2                       | 39.0                        | 34.9                          |
| 26DCzppy | 88                       | 17                        | 4.1                      | 40.2                       | 38.1                        | 32.4                          |

<sup>a</sup> PLQY of spin coated film doped with 10 wt% Firpic in host, measured using an integrating sphere. <sup>b</sup> Measured at  $1 \text{ cd m}^{-2}$ .

## Summary

A series of phenanthro[9,10-*d*]imidazole/triazole host materials were developed as alternative non-carbazole hosts for blue PHOLEDs. The synthesis, photophysics and electrochemical properties of N2 and N1-aryl substituted phenanthro[9,10-*d*]triazoles are described. The materials exhibit wide energy gaps and triplet energies as high as 2.97 eV, which are crucial parameters for use as hosts for blue PHOLEDs. The triplet energies undergo a marked redshift of *ca.* 0.30 eV in the solid state compared to values in solution. To partially overcome aggregation effects, bulky substituent groups were incorporated

into the 1-position, reducing the red shift in the solid state to 0.1 eV. The triplet energy in the solid state is sufficiently high to host cyan-emitting FIrpic with a PLQY of near unity. Furthermore, these materials exhibit moderate glass transition temperatures with no decomposition observed during sublimation.

The optimized materials were incorporated as host materials for blue OLEDs, showing similar transport properties as *mCBP*. Devices using phenanthro-triazole host materials exhibited a maximum EQE of 21%, although they were quite unstable. In contrast, devices using phenanthro-imidazole hosts showed a maximum EQE of 20% and a roll-off similar to an *mCBP* hosted device, indicating improved stability of these materials. Therefore, the phenanthro-imidazole hosts can serve as alternatives to carbazole-based host materials for OLEDs using blue phosphorescent and thermally activated delayed fluorescent (TADF) emitters.

## Conflicts of interest

Two of the authors (M. E. T and S. R. F.) have a financial interest in one of the sponsors of this work, *i.e.* Universal Display Corporation.

## Acknowledgements

The authors thank the Department of Energy, Office of Energy Efficiency and Renewable Energy (Grant #: DE-EE0007077), US Air Force Office of Scientific Research (Grant #: DE-EE0007626) and the Universal Display Corporation for their financial support of this work.

## References

- (a) C. W. Tang and S. A. VanSlyke, Organic electroluminescent diodes, *Appl. Phys. Lett.*, 1987, **51**(12), 913–915; (b) S.-J. Su, C. Cai and J. Kido, RGB Phosphorescent Organic Light-Emitting Diodes by Using Host Materials with Heterocyclic Cores: Effect of Nitrogen Atom Orientations, *Chem. Mater.*, 2011, **23**(2), 274–284; (c) S.-C. Dong, L. Zhang, J. Liang, L.-S. Cui, Q. Li, Z.-Q. Jiang and L.-S. Liao, Rational Design of Dibenzothiophene-Based Host Materials for PHOLEDs, *J. Phys. Chem. C*, 2014, **118**(5), 2375–2384.
- (a) X. Ren, J. Li, R. J. Holmes, P. I. Djurovich, S. R. Forrest and M. E. Thompson, Ultrahigh Energy Gap Hosts in Deep Blue Organic Electrophosphorescent Devices, *Chem. Mater.*, 2004, **16**(23), 4743–4747; (b) D. F. O'Brien, M. A. Baldo, M. E. Thompson and S. R. Forrest, Improved energy transfer in electrophosphorescent devices, *Appl. Phys. Lett.*, 1999, **74**(3), 442–444; (c) P. E. Burrows, S. R. Forrest, T. X. Zhou and L. Michalski, Operating lifetime of phosphorescent organic light emitting devices, *Appl. Phys. Lett.*, 2000, **76**(18), 2493–2495; (d) V. Adamovich, J. Brooks, A. Tamayo, A. M. Alexander, P. I. Djurovich, B. W. D'Andrade, C. Adachi, S. R. Forrest and M. E. Thompson, High efficiency single dopant white electrophosphorescent light emitting diodes, *New J. Chem.*, 2002, **26**(9), 1171–1178.
- (a) C. W. Tang, Two-layer organic photovoltaic cell, *Appl. Phys. Lett.*, 1986, **48**(2), 183–185; (b) J. J. Chen, S. M. Conron, P. Erwin, M. Dimitriou, K. McAlahney and M. E. Thompson, High-Efficiency BODIPY-Based Organic Photovoltaics, *ACS Appl. Mater. Interfaces*, 2015, **7**(1), 662–669.
- (a) M. Kitamura and Y. Arakawa, Current-gain cutoff frequencies above 10 MHz for organic thin-film transistors with high mobility and low parasitic capacitance, *Appl. Phys. Lett.*, 2009, **95**(2), 023503; (b) U. Zschieschang, V. P. Bader and H. Klauk, Below-one-volt organic thin-film transistors with large on/off current ratios, *Org. Electron.*, 2017, **49**, 179–186.
- (a) M. Alfonso, A. Espinosa, A. Tárraga and P. Molina, Multifunctional Benzothiadiazole-Based Small Molecules Displaying Solvatochromism and Sensing Properties toward Nitroarenes, Anions, and Cations, *ChemistryOpen*, 2014, **3**(6), 242–249; (b) B. Kulyk, S. Taboukhat, H. Akdas-Kilig, J.-L. Fillaut, M. Karpierz and B. Sahraoui, Tuning the non-linear optical properties of BODIPYs by functionalization with dimethylaminostyryl substituents, *Dyes Pigm.*, 2017, **137**, 507–511.
- (a) T. Tsujimura, New OLED Applications, in *OLED Display Fundamentals and Applications*, ed. A. C. Lowe and I. Sage, 2017; (b) C. Coburn, C. Jeong and S. R. Forrest, Reliable, All-Phosphorescent Stacked White Organic Light Emitting Devices with a High Color Rendering Index, *ACS Photonics*, 2018, **5**(2), 630–635; (c) F. So, J. Kido and P. Burrows, Organic Light-Emitting Devices for Solid-State Lighting, *MRS Bull.*, 2008, **33**(7), 663–669.
- (a) M. A. Baldo, D. F. O'Brien, Y. You, A. Shoustikov, S. Sibley, M. E. Thompson and S. R. Forrest, Highly efficient phosphorescent emission from organic electroluminescent devices, *Nature*, 1998, **395**, 151; (b) M. A. Baldo, S. Lamansky, P. E. Burrows, M. E. Thompson and S. R. Forrest, Very high-efficiency green organic light-emitting devices based on electrophosphorescence, *Appl. Phys. Lett.*, 1999, **75**(1), 4–6; (c) C. Adachi, R. C. Kwong, P. Djurovich, V. Adamovich, M. A. Baldo, M. E. Thompson and S. R. Forrest, Endothermic energy transfer: a mechanism for generating very efficient high-energy phosphorescent emission in organic materials, *Appl. Phys. Lett.*, 2001, **79**(13), 2082–2084; (d) C. Adachi, M. A. Baldo, M. E. Thompson and S. R. Forrest, Nearly 100% internal phosphorescence efficiency in an organic light-emitting device, *J. Appl. Phys.*, 2001, **90**(10), 5048–5051.
- (a) R. J. Holmes, S. R. Forrest, Y. J. Tung, R. C. Kwong, J. J. Brown, S. Garon and M. E. Thompson, Blue organic electrophosphorescence using exothermic host-guest energy transfer, *Appl. Phys. Lett.*, 2003, **82**(15), 2422–2424; (b) S. Tokito, T. Iijima, Y. Suzuri, H. Kita, T. Tsuzuki and F. Sato, Confinement of triplet energy on phosphorescent molecules for highly-efficient organic blue-light-emitting devices, *Appl. Phys. Lett.*, 2003, **83**(3), 569–571.
- (a) C. W. Lee and J. Y. Lee, Above 30% External Quantum Efficiency in Blue Phosphorescent Organic Light-Emitting Diodes Using Pyrido[2,3-*b*]indole Derivatives as Host Materials, *Adv. Mater.*, 2013, **25**(38), 5450–5454; (b) S. Y. Byeon, J. H. Kim and J. Y. Lee, CN-Modified Host Materials for Improved Efficiency and Lifetime in Blue Phosphorescent and Thermally Activated Delayed Fluorescent Organic Light-Emitting Diodes,

- ACS Appl. Mater. Interfaces*, 2017, **9**(15), 13339–13346; (c) M. M. Rothmann, S. Haneder, E. Da Como, C. Lennartz, C. Schildknecht and P. Strohriegl, Donor-Substituted 1,3,5-Triazines as Host Materials for Blue Phosphorescent Organic Light-Emitting Diodes, *Chem. Mater.*, 2010, **22**(7), 2403–2410.
- 10 Y.-H. Chen, H.-H. Chou, T.-H. Su, P.-Y. Chou, F.-I. Wu and C.-H. Cheng, Synthesis and photo- and electroluminescence properties of 3,6-disubstituted phenanthrenes: alternative host material for blue fluorophores, *Chem. Commun.*, 2011, **47**(31), 8865–8867.
- 11 (a) H. Huang, Y. Wang, S. Zhuang, X. Yang, L. Wang and C. Yang, Simple Phenanthroimidazole/Carbazole Hybrid Bipolar Host Materials for Highly Efficient Green and Yellow Phosphorescent Organic Light-Emitting Diodes, *J. Phys. Chem. C*, 2012, **116**(36), 19458–19466; (b) K. Togashi, T. Yasuda and C. Adachi, Triphenylene-based Host Materials for Low-voltage, Highly Efficient Red Phosphorescent Organic Light-emitting Diodes, *Chem. Lett.*, 2013, **42**(4), 383–385.
- 12 S. Chen, Y. Wu, Y. Zhao and D. Fang, Deep blue organic light-emitting devices enabled by bipolar phenanthro[9,10-*d*]imidazole derivatives, *RSC Adv.*, 2015, **5**(88), 72009–72018.
- 13 M. R. Daniel Sylvinson, H. F. Chen, L. M. Martin, P. J. G. Saris and M. E. Thompson, Rapid Multiscale Computational Screening for OLED Host Materials, *ACS Appl. Mater. Interfaces*, 2019, **11**(5), 5276–5288.
- 14 (a) G. Yasuda and H. Kimoto, Substitution reactions of phenanthro[9,10-*d*]triazole with benzyl chlorides, *J. Heterocycl. Chem.*, 2009, **35**(2), 365–369; (b) A. A. Taherpour and M. Faraji, One-pot Microwave-Assisted Synthesis of 1*H*-Phenanthro[9,10-*d*][1,2,3]triazole, *Molbank*, 2008, **2008**(3), M577; (c) N. S. Mani and A. E. Fitzgerald, A Step-Economical Route to Fused 1,2,3-Triazoles via an Intramolecular 1,3-Dipolar Cycloaddition between a Nitrile and an *in Situ* Generated Aryldiazomethane, *J. Org. Chem.*, 2014, **79**(18), 8889–8894.
- 15 (a) S. Ueda, M. Su and L. Buchwald Stephen, Highly N2-Selective Palladium-Catalyzed Arylation of 1,2,3-Triazoles, *Angew. Chem., Int. Ed.*, 2011, **50**(38), 8944–8947; (b) M. Taillefer, N. Xia and A. Ouali, Efficient Iron/Copper Co-Catalyzed Arylation of Nitrogen Nucleophiles, *Angew. Chem., Int. Ed.*, 2007, **46**(6), 934–936.
- 16 Q. Chen, H. Yu, Z. Xu, L. Lin, X. Jiang and R. Wang, Development and Application of *O*-(Trimethylsilyl)aryl Fluoro-sulfates for the Synthesis of Arynes, *J. Org. Chem.*, 2015, **80**(13), 6890–6896.
- 17 A. F. Rausch, M. E. Thompson and H. Yersin, Blue Light Emitting Ir(III) Compounds for OLEDs – New Insights into Ancillary Ligand Effects on the Emitting Triplet State, *J. Phys. Chem. A*, 2009, **113**(20), 5927–5932.
- 18 G. A. George and D. K. C. Hodgeman, Quantitative phosphorescence spectroscopy of polystyrene during photo-degradation and the significance of in-chain peroxides, *Eur. Polym. J.*, 1977, **13**(1), 63–71.
- 19 J. Sworakowski, J. Lipiński and K. Janus, On the reliability of determination of energies of HOMO and LUMO levels in organic semiconductors from electrochemical measurements. A simple picture based on the electrostatic model, *Org. Electron.*, 2016, **33**, 300–310.
- 20 E. Baranoff, B. F. E. Curchod, F. Monti, F. Steimer, G. Accorsi, I. Tavernelli, U. Rothlisberger, R. Scopelliti, M. Grätzel and M. K. Nazeeruddin, Influence of Halogen Atoms on a Homologous Series of Bis-Cyclometalated Iridium(III) Complexes, *Inorg. Chem.*, 2012, **51**(2), 799–811.